Lateral composition modulation in AlAs/InAs short period superlattices grown on InP(001)

J. Mirecki Millunchick, R. D. Twesten, D. M. Follstaedt, S. R. Lee, E. D. Jones, Yong Zhang, S. P. Ahrenkiel, and A. Mascarenhas

Citation: Appl. Phys. Lett. **70**, 1402 (1997); doi: 10.1063/1.118589
View online: https://doi.org/10.1063/1.118589
View Table of Contents: http://aip.scitation.org/toc/apl/70/11
Published by the American Institute of Physics

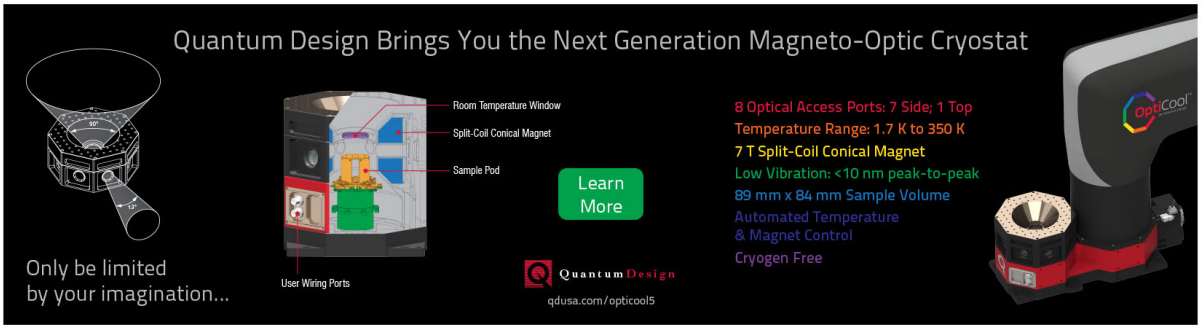

Lateral composition modulation in AlAs/InAs short period superlattices grown on InP(001)

J. Mirecki Millunchick, R. D. Twesten, D. M. Follstaedt, S. R. Lee, and E. D. Jones
Sandia National Laboratory, Albuquerque, New Mexico 87185

Yong Zhang, S. P. Ahrenkiel, and A. Mascarenhas
National Renewable Energy Laboratory, Golden, Colorado 80401

(Received 13 November 1996; accepted for publication 13 January 1997)

Spontaneous lateral composition modulation as a consequence of the deposition of a $(AlAs)_n/(InAs)_m$ short period superlattice on an InP(001) substrate is examined. Transmission electron microscopy images show distinct composition modulation appearing as vertical regions of In- and Al-rich materials alternating in the [110] projection. The periodicity of the modulation is 130 Å, and is asymmetric. The transmission electron and x-ray diffraction patterns from the structure exhibit distinct satellite spots which correspond to the lateral periodicity. Transmission electron microscopy images show that the individual superlattice layers possess cusplike undulations, which directly correlate with the composition modulation. Composition modulation in this sample appears to be coupled to morphological and compositional instabilities at the surface due to strain. © *1997 American Institute of Physics.* [S0003-6951(97)04111-9]

Recently, there has been a great impetus to apply low-dimensional structures to novel electronic and photonic devices.[1] For example, lasers with quantum wire (QWR) active regions are predicted to have lower threshold currents, wider modulation bandwidths, and better temperature stability.[1] Deposition of short period superlattices (SPS) of InAs/GaAs[2] and InP/GaP[3] by molecular beam epitaxy (MBE) has been shown to result in lateral composition modulation, which has been exploited to obtain high densities of nanometer-sized QWR, without the processing limitations of other fabrication methods. Application of this technique to the InAlAs system, an important wide-band-gap material in high-speed electronics and optoelectronics,[4] can lead to novel polarization-sensitive devices. In a laser structure, for example, cladding layers consisting of AlAs/InAs SPS can produce QWR behavior in active layers of InGaAs due to composition-modulation induced strain fields.[5] In this letter, we report the growth of a $(AlAs)_n/(InAs)_m$/InP(001) SPS that has spontaneously formed lateral composition modulation.

The growth of the SPS was performed on a *n*-type InP(001) substrate by MBE. A 1.0-μm-thick buffer layer of $In_{0.5}Al_{0.5}As$ was deposited at a substrate temperature 530 °C and a growth rate $R=0.685$ monolayers per second (ML/s), as calibrated by reflection high energy electron diffraction. Next, an undoped $(AlAs)_n/(InAs)_m$ SPS was deposited with n and m less than the critical thickness of AlAs/InAs, ≈ 2 ML. Double-crystal x-ray diffraction confirmed that the average indium composition x of the buffer layer was $x=0.50$, and $x=0.46$ for the SPS structure. The superlattice period was found to be 3.35 ML by transmission electron microscopy. Therefore, the thickness of the individual superlattice layers averaged over the entire SPS structure was $n=1.9$ and $m=1.6$ ML. Polarized photoluminescence measurements at 10 K were performed in order to investigate the optical properties of the structure. The spectra from the SPS showed that the intensity of the photoluminescence was polarized with respect to the composition modulation, in agreement with other published results.[2,3,6,12]

Figure 1 shows transmission electron microscopy (TEM) images recorded at 200 kV for both the [110] and [1$\bar{1}$0] projections. In addition to the contrast arising from the SPS periodicity, the bright- and dark-field (002) images both show a strong, regular lateral contrast modulation(perpendicular to the growth direction) in the [110] projection [Figs. 1(a) and 1(b)] but not in the [1$\bar{1}$0] projection [Fig. 1(c)]. Since the (002) structure factor is very sensitive to the local composition but not lateral strain, we attribute the image contrast to modulation in the local group III composition. This interpretation is supported by dark-field (004) images (not shown) which are only weakly affected by local composition variations, and do not show lateral contrast variations. Any shear strains resulting from composition modulation wave in the (110) directions will not be visible in either (002) or (004) images.[7] The contrast in the (002) bright-field image in the [110] projection [Fig. 1(a)] is highly asymmetric, with narrow dark regions separated by wide light regions. In the (002) dark-field image of the same projection [Fig. 1(b)], these narrow regions appear as thin black bands surrounding much lighter centers. This contrast is a result of the extinction of the (002) structure factor when the local In composition reaches $\sim$52%.[8] Therefore, we can deduce that the narrow region is In rich with $x>0.52$. This interpretation is supported by [110] zone axis lattice images (not shown) showing tetragonal expansion of the [110] planes in these regions. The average modulation wavelength is measured to be $\sim$130 Å and this is also borne out in diffraction patterns (see below). Other films grown under similar conditions also exhibit contrast variations due to composition modulation.

Bright-field (002) images [Figs. 1(a) and 1(c)] clearly show the individual InAs/AlAs SPS layers. For the [1$\bar{1}$0] projection, [Fig. 1(c)], the layers are flat, while in the [110] projection [Fig. 1(a)], the SPS layers show sharp cusplike undulations. These cusps do not appear in the SPS until approximately the seventh period of the superlattice, testifying that they did not originate in the buffer layer but began in the SPS. The cusps indicate the growth front was not atomically smooth during deposition of the SPS. The position of these

 0003-6951/97/70(11)/1402/3/$10.00

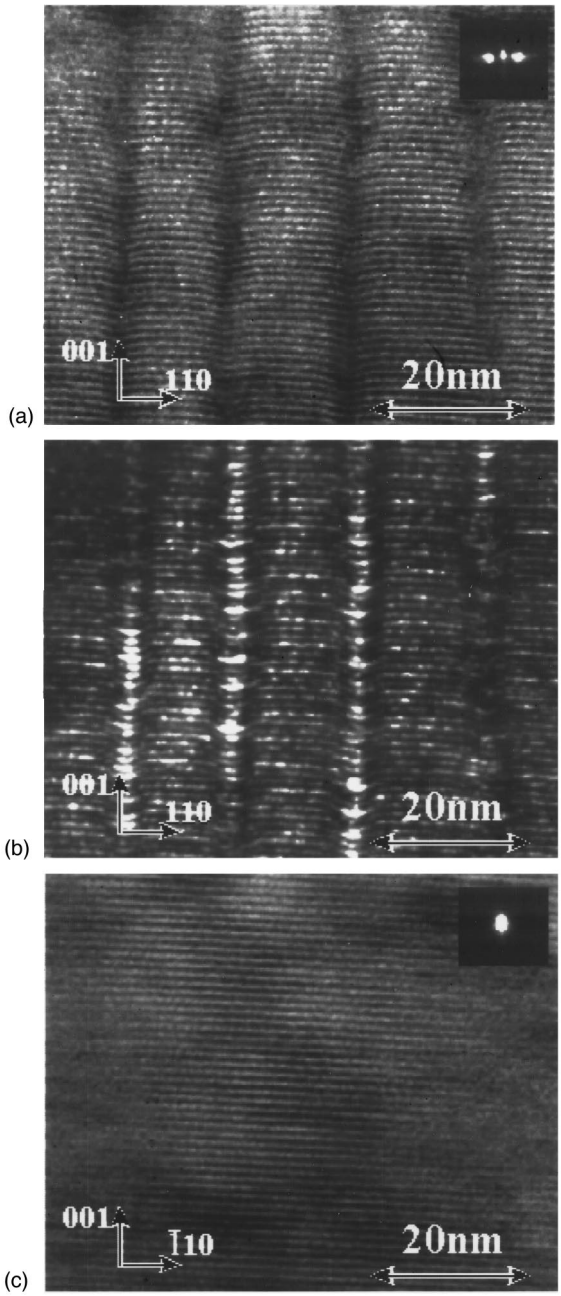

FIG. 1. TEM images of the SPS structure in the $[\bar{1}10]$ (a,b) and the [110] projections. (a) Bright-field (002) image in the [110] projection showing the individual layers of the SPS. The layers show cusplike undulations indicating a nonplanar growth front [compare to Fig. 2(c)]. Inset: (002) diffraction spots showing lateral satellites. (b) Dark-field 002 image of the area in (a). The regular, lateral contrast is due to modulation of the local Al/In ratio. The narrow bright region between the dark bands is the center of the In-rich region while the broader bright region is Al rich. (c) Bright-fields $g=002$ image in the [110] projection. Note the lack of both lateral contrast and cusps in the SPS. Inset: (002) diffraction spot with no lateral satellites.

cusps correspond to maximum In concentration in the lateral modulation as seen in Fig. 1(b). This is consistent with the expected strain relief of a nonplanar film in tension.[9,15]

The directionality of the composition modulation occurs due to the anisotropy of the As-stabilized surface structure. It is well known that for III–V's under high group-V overpressure, the surface reconstruction consists of group-V dimers elongated in the [110] direction. In the absence of step flow,

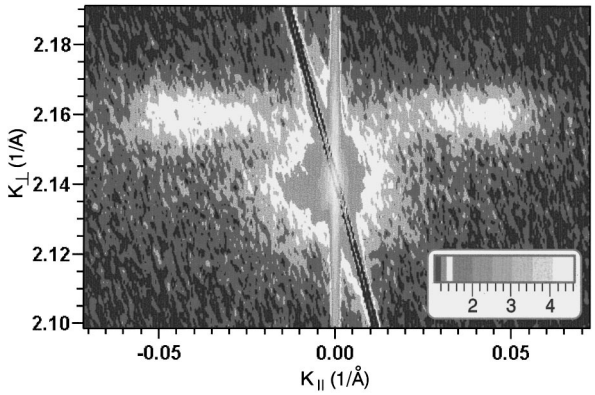

FIG. 2. The reciprocal space map of the (002) spot in the $[\bar{1}10]$ projection.

growth proceeds by the nucleation, growth, and coalescence of 2D islands elongated along the [110] direction. Composition modulation occurs along the perpendicular direction.

The (002) transmission electron diffraction (TED) spots for the SPS in the two $\langle 110 \rangle$ directions are shown in the insets of Figs. 1(a) and 1(c). Distinct lateral satellites on either side of the principle diffraction spot are clearly visible in [110] projection, corresponding to a periodicity of 130 Å. The diffraction spot in the orthogonal projection does not show distinct satellites. Satellites are also visible above and below the principle diffraction spot which correspond to the SPS periodicity. Figure 2 shows an x-ray diffraction reciprocal space map of the (002) diffraction spot in the [110] projection. Again, sharp and distinct lateral satellites are visible, in agreement with the TED results. The reciprocal space map also shows that the SPS peak and satellites are in tension, in agreement with the double crystal x-ray diffraction results.

Composition modulation has been attributed to a number of different mechanisms. A common explanation is that it is a thermodynamic effect; i.e., the alloy experiences spinodal decomposition.[10] However, typical growth conditions are generally above the chemical spinodal, the condition where the second derivative of the free energy with respect to composition is positive, and well above the coherent spinodal. The coherent strain between components of the alloy tends to stabilize the solution to fluctuations in composition, thus significantly suppressing the critical temperature for spinodal decomposition.[11] Furthermore, spinodal decomposition is a bulk effect, whereas composition modulation is clearly established as a surface phenomenon. The reasons are as follows: (i) the asymmetry between the [110] and $[\bar{1}10]$ can only be explained by the dimerization of the surface, and (ii) the cusps, which indicate the nonplanarity of the growth front, correlate with the In-rich layers as seen in Fig. 1. For systems that exhibit composition modulation in SPS,[2,3,12] strain resulting from deviations from lattice matching between the individual superlattice layers has been cited as a mechanism that initiates lateral composition modulation. This work illustrates that composition modulation appears directly correlated with the morphology of the growth front.

For a strained film, a nonplanar surface is more stable than a flat one.[13] The presence of a surface corrugation can relieve strain by allowing portions of the surface to relax. One source of undulation-producing strain originates from

lattice mismatch, the difference in the lattice parameter between the substrate and film. The same factors that drive morphological stability also affect compositional stability in alloys.[14–16] In the presence of strain, the composition of the alloy will vary along the undulation direction because large atoms preferentially nucleate where the lattice is dilated, and smaller atoms where the lattice is compressed. In this work, TEM images show that the morphology of the SPS layers are undulated, and that the composition varies along the undulation. Several theories[14–16] describe surface undulations as related to composition modulation for alloys, however, they may not be directly applicable to an SPS structure.

In conclusion, we have investigated composition modulation in a $(AlAs)_n/(InAs)_m$ short period superlattice grown on a InP(001). The modulation only appeared in the [110] projection, with a periodicity of 130 Å. The diffraction pattern of the structure, as seen in TED and reciprocal space mapping, exhibited distinct satellite spots which correspond to the lateral periodicity. The TEM images have shown that the SPS layers possess cusplike undulation, which directly correlated to the composition modulation. Therefore, composition modulation is attributed to morphological and compositional instabilities at the surface due to strain.

The authors wish to thank J. E. Guyer and P. W. Voorhees for many useful discussions, and gratefully acknowledge the support of the U.S. Department of Energy, OER/BES Division of Materials Science under Grant No. DE-AC02-83-CH10093.

[1] C. Weisbuch and B. Vinter, *Quantum Semiconductor Structures: Fundamentals and Applications*, (Academic, New York, 1991).
[2] S. T. Chou, K. Y. Cheng, L. J. Chou, and K. C. Hseih, J. Appl. Phys. **78**, 6270 (1995).
[3] A. C. Chen, A. M. Moy, L. J. Chou, K. C. Hsieh, and K. Y. Cheng, Appl. Phys. Lett. **66**, 2694 (1995).
[4] P. Abraham, M. A. Garcia Perez, T. Benyattou, G. Guilot, M. Sacilotti, and X. Letartre, Semicond. Sci. Technol. **10**, 1585 (1995).
[5] F. Peiro, A. Cornet, J. C. Ferrer, J. R. Merante, G. Halkias, and A. Georgakilas, *Materials Research Society Symposium Proceedings*, edited by E. D. Jones, A. Mascarenhas, and P. Petroff (Materials Research Society, Pittsburgh, 1996), p. 265.
[6] A. Mascarenhas, R. G. Alonso, G. S. Horner, S. Froyen, K. C. Hsieh, and K. Y. Cheng, Superlattices Microstruct. **12**, 57 (1992).
[7] M. M. J. Treacy, J. M. Gibson, and A. Howie, Philos. Mag. A **51**, 389 (1985).
[8] At an In composition of 52%, the average scattering factor for the In and Al exactly equals the As scattering factor resulting in zero contrast for the (002) structure factor. See for example, M. A. Hirsch, A. Howie, R. Nicholson, D. W. Pashley, and M. J. Whelan, Electron Microscopy of Thin Crystals, 1967 (unpublished).
[9] For a compressively strained film, the peaks of the undulation will relax to a larger lattice parameter than in the valleys, as seen in Fig. 1 of A. G. Cullis, MRS Bull. 21 (1996). The reverse is true for a tensilely strained film, i.e., the peaks will relax to a smaller lattice parameter.
[10] J. E. Oh, P. K. Bhattacharya, Y. C. Chen, O. Aina, and M. Mattingly, J. Electron. Mater. **19**, 435 (1990).
[11] J. W. Cahn, Acta Metall. **9**, 975 (1961).
[12] K. Y. Cheng, K. C. Hsieh, and J. N. Baillargeon, Appl. Phys. Lett. **60**, 2892 (1992).
[13] D. J. Srolovitz, Acta Metall. **37**, 621 (1989).
[14] J. Tersoff, Phys. Rev. Lett. **77**, 2017 (1996).
[15] J. E. Guyer and P. W. Voorhees, Phys. Rev. B **54**, 11 710 (1996).
[16] F. Glas, J. Appl. Phys. **62**, 3201 (1987).